19. W. A. Dziembowski, A. A. Pamjatnykh, R. Sienkiewicz, *Mon. Not. R. Astron. Soc.* **249**, 602 (1991); W. Däppen *et al.*, in *Challenges to Theories of the Structure of Moderate-Mass Stars*, D. O. Gough and J. Toomre, Eds. (Lecture Notes in Physics 388, Springer, Heidelberg, Germany, 1991), pp. 111–120. A. Kosovichev *et al., Mon. Not. R. Atron. Soc.* **259**, 536 (1992); H. M. Antia and S. Basu, *Astrophys. J.* **426**, 801 (1994); A. G. Kosovichev, *Adv. Space Res.* **15**, 95 (1995).
20. M. J. Thompson *et al.*, *Science* **272**, 1300 (1996).
21. The wave is also advected by azimuthal flow, but the axisymmetric component of that flow is rotation, which is addressed in (*20*).
22. E. G. Zweibel and D. O Gough, in *Procedings of the Fourth SOHO Workshop: Helioseismology*, J. T. Hoeksema *et al.*, Eds. [European Space Agency (ESA) Special Publication (SP)–379, Noordwijk, Netherlands, 1995]. Although one cannot distiguish between possible sources of asphericity by analyzing frequencies alone, the different anisotropies of the wave-speed perturbations from different sources renders it possible in principle to distinguish them by their eigenfunctions. That might be possible in the future with the use of techniques such as time-distance seismology.
23. The averaging kernels in this case are quadratic in the horizontal structure of the eigenfunctions. They are therefore even functions of latitude and are sensitive only to the north-south symmetric component of the asphericity. It requires some knowledge of the form of the eigenfunctions to determine the asymmetric component.
24. D. O. Gough and M. J. Thompson, in *Advances in Helio- and Asteroseismology*, J. Christensen-Dalsgaard and S. Frandsen, Eds. (Reidel, Dordrecht, Netherlands, 1988), pp. 175–180; J. R. Kuhn, *Astrophys. J. Lett.* **331**, L131 (1988); P. R. Goode and J. R. Kuhn, *Astrophys. J.* **356**, 310 (1990); K. G. Libbrecht and M. F. Woodard, *ibid.* **402**, L77 (1993).
25. E. A. Spiegel and N. O. Weiss, *Nature* **287**, 616 (1980); C. A. Morrow, P. A. Gilman, E. E. DeLuca, in *Seismology of the Sun and Sun-Like Stars*, V. Domingo and E. J. Rolfe, Eds. (ESA SP-286, Noordwijk, Netherlands, 1988), vol. 2, pp. 73–76; S. Moreno-Insertis, in *Sunspots: Theory and Observation*, J. H. Thomas and N. O. Weiss, Eds. (Kluwer, Dordrecht, Netherlands, 1994).
26. D. O. Gough and T. Sekii, *Astron. Soc. Pac. Conf. Ser.* **42**, 177 (1993); M. J. P. F. G. Monteiro, J. Christensen-Dalsgaard, M. J. Thompson, *ibid.*, p. 253; A. G. Kosovichev, in *Advances in Solar Physics*, Proceedings of the Seventh European Meeting on Solar Physics, G. Belvedere, M. Rodono, G. M. Simnett, Eds. (Lecture Notes in Physics 432, Springer-Verlag, Germany, 1994), pp. 47–52; S. Basu and H. M. Antia, *Mon. Not. R. Astron. Soc.* **269**, 1137 (1995).
27. D. O. Gough, in *Solar-Terrestrial Relationships and the Earth Environment in the Last Millenia*, G. Castagnoli-Cini, Ed. (Italiana Fisica, Bologna, Italy, 1988), pp. 90–132 ; E. Knobloch and W. J. Merryfield, *Astrophys. J.* **401**, 196 (1992).
28. J.-P.Zahn, *Astron. Astrophys.* **265**, 115 (1992).
29. E. A. Spiegel and J.-P. Zahn, *ibid.*, p. 106.
30. We have investigated the structure of the transition between the convection zone and the radiative interior by first considering how mode frequency varies with the phase difference between the surface of the sun and the base of the convection zone, after having filtered out surface effects, and then comparing it with theoretical models (*32*). The signature of the transition oscillates with phase, in step with the eigenfunctions, with an amplitude that is smaller than that of the reference model, confirming that, if spherical, the transition is smoother than that of the model. The apparent smoothness might have come about because what has been observed is actually the spherical average of an aspherical structure. Adiabatic convective overshooting is likely to increase the amplitude; therefore, if such overshooting occurs in the sun, the physical discrepancy is actually greater than it appears at first sight. There is some indication that the amplitude of the oscillatory signal varies with the ratio m/ℓ of azimuthal order to degree. This suggests that the structure of the lower boundary layer of the convection zone might vary with latitude. Although at present this is no more than a hint, it points to an exciting direction of research with further long-term seismic data.
31. J. N. Bahcall and H. A. Bethe, *Phys. Rev.* **D47**, 1298 (1993)
32. M. J. P. F. G. Monteiro and M. J. Thompson, *Astron. Astrophys.* **283**, 247 (1994), J. Christensen-Dalsgaard, M. J. P. F. G. Monteiro, M. J. Thompson, *Mon. Not. R. Astron. Soc.* **276**, 283 (1995); I. W. Roxburgh and S. V. Vorontsov, *ibid.* **268**, 880 (1994); S. Basu, H. M. Antia, D. Narasimha, *ibid.* **267**, 207 (1994).

33. GONG is managed by the National Solar Observatory, a division of the National Optical Astronomy Observatories, operated by AURA under a cooperative agreement with NSF. We acknowledge financial support from the U.K. Particle Physics and Astronomy Research Council, NSF, NASA, and Danmarks Grundforskningsfond.

18 March 1996; accepted 9 May 1996

Differential Rotation and Dynamics of the Solar Interior

M. J. Thompson, J. Toomre, E. R. Anderson, H. M. Antia, G. Berthomieu, D. Burtonclay, S. M. Chitre, J. Christensen-Dalsgaard, T. Corbard, M. DeRosa, C. R. Genovese, D. O. Gough, D. A. Haber, J. W. Harvey, F. Hill, R. Howe, S. G. Korzennik, A. G. Kosovichev, J. W. Leibacher, F. P. Pijpers, J. Provost, E. J. Rhodes Jr., J. Schou, T. Sekii, P. B. Stark, P. R. Wilson

Splitting of the sun's global oscillation frequencies by large-scale flows can be used to investigate how rotation varies with radius and latitude within the solar interior. The nearly uninterrupted observations by the Global Oscillation Network Group (GONG) yield oscillation power spectra with high duty cycles and high signal-to-noise ratios. Frequency splittings derived from GONG observations confirm that the variation of rotation rate with latitude seen at the surface carries through much of the convection zone, at the base of which is an adjustment layer leading to latitudinally independent rotation at greater depths. A distinctive shear layer just below the surface is discernible at low to mid-latitudes.

On the time scale of stellar evolution, the sun is a middle-aged star. The observed surface rotation rates of young solar-type stars are up to 50 times that of the sun. It is therefore believed that the sun has been losing angular momentum over its lifetime through its magnetized wind, thereby gradually spinning down its outer convection zone and probably the bulk of its interior. The effectiveness of the overall spin-down of the star is difficult to estimate from stellar evolution theory, because delicately balanced circulations and instabilities that would tend to mix the interior—and magnetic fields that may retard or modify such processes—must be taken into account (*1*). This has led to suggestions that the sun might still have a rapidly rotating core, perhaps highly magnetized, reflecting its primordial past. The apparent deficit of neutrinos coming from the sun's energy-generating core has also prompted ideas for readjusting the chemical composition and stratification in models of the nuclear-burning core, and such adjustments have implications for the mixing of angular momentum in that region (*2*). Tracking of surface features has shown that the sun does not rotate as a solid body: it rotates once in ~25 days near the equator and in ~33 days near the poles. Further, the rotation rate of sunspots at low and mid-latitudes is somewhat faster than that deduced from Doppler shifts of the surface plasma; this finding suggests that the magnetic fields of the spots may be

M. J. Thompson and R. Howe are in the Astronomy Unit, Queen Mary and Westfield College, University of London, Mile End Road, London E1 4NS, UK. J. Toomre, M. DeRosa, and D. A. Haber are at the Joint Institute for Laboratory Astrophysics, University of Colorado, Boulder, CO 80309–0440, USA. E. R. Anderson, J. W. Harvey, F. Hill, and J. W. Leibacher are at the National Solar Observatory (NSO), National Optical Astronomy Observatories (NOAO), Post Office Box 26732, Tucson, AZ 85726–6732, USA. H. M. Antia and S. M. Chitre are at the Tata Institute of Fundamental Research, Bombay 400005, India. G. Berthomieu, T. Corbard, and J. Provost are at the Observatoire de la Cote d'Azur, 06304 Nice Cedex 4, France. D. Burtonclay and P. R. Wilson are in the School of Mathematics, University of Sydney, Sydney, NSW 2006, Australia. J. Christensen-Dalsgaard and F. P. Pijpers are at the Theoretical Astrophysics Center, Aarhus University, DK-8000 Aarhus C, Denmark. C. R. Genovese is in the Department of Statistics, Carnegie Mellon University, Pittsburgh, PA 15213, USA. D. O. Gough and T. Sekii are in the Institute of Astronomy, University of Cambridge, Cambridge CB3 0HA, UK. S. G. Korzennik is at the Harvard-Smithsonian Center for Astrophysics, 60 Garden Street, Cambridge, MA 02138, USA. A. G. Kosovichev and J. Schou are at Hansen Experimental Physics Laboratory Annex, Stanford University, Stanford, CA 94305–4085, USA. E. J. Rhodes Jr. is in the Department of Physics and Astronomy, University of Southern California, Los Angeles, CA 90089, USA. P. B. Stark is in the Department of Statistics, University of California, Berkeley, CA 94720–3860, USA.

rooted to more rapidly rotating plasma deeper in the convection zone, which occupies the sun's outer 30% by radius (3).

Theoretical studies indicate that turbulent compressible convection couples with rotation to redistribute the angular momentum away from simple solid-body rotation, leading to differential rotation and meridional circulations. Moreover, the interplay of turbulent motions and rotation with magnetic fields is generally believed to be responsible for magnetic dynamo action that leads to the observed 22-year cycles of sunspots and solar magnetic activity (4). During the past decade, helioseismology has begun to provide the means to estimate the rotation profile of the interior of the sun. The helioseismic findings are not compatible with the predictions of most theoretical models of the rotation profile set up by turbulent convection in the sun's envelope (5), which raises serious doubts about our current understanding of global-scale solar convection. Here, we use the nearly continuous GONG observations to probe the dynamical state of the solar convection zone and the deeper radiative interior.

The horizontal structure of each global mode of oscillation of the sun is described by a spherical harmonic Y_ℓ^m of degree ℓ and order m, and the vertical structure is described by ℓ and the radial order n. Opposite signs of m correspond to modes propagating in opposite directions around the sun's equator. In a spherically symmetric star, the frequencies depend on n and ℓ but not on m, so for each (n,ℓ) pair there is a $(2\ell + 1)$-fold degeneracy. Rotation breaks the spherical symmetry and lifts the degeneracy. Advection causes a wave propagating with the sun's rotation to have a higher measured frequency than would a similar wave propagating against the rotation. The difference in frequency of a pair of oppositely propagating modes is proportional to m times a weighted average of the rotation rate $\Omega(r,\theta)$ in the region of radius r and latitude θ where the modes have appreciable amplitude. We define the frequency splitting $\Delta\nu_{n\ell m}$ to be half the value of this difference. Each frequency splitting measures a longitudinal and temporal average of the zonal flows over the period of the observations (6). Different modes have different spatial sensitivity, so the observed frequency splittings can be used to make inferences about spatial variations in Ω.

There were several early attempts (7, 8) to measure rotational splittings, but the first definitive results yielding estimates of Ω over a range of depths were obtained from observation of intermediate-degree sectoral ($m = \pm\ell$) modes (9). The frequency splittings yielded inferences for Ω close to the equatorial plane, which suggested that much of the interior of the sun rotates slightly less rapidly than does the surface, whereas the central region appears to rotate more rapidly. Such data also indicated that the quadrupole moment J_2 of the sun's exterior gravitational field is consistent with general relativity. These studies were soon followed by full-disk imaging observations that yielded information on a wide variety of tesseral ($0 < |m| < \ell$) modes, thereby providing estimates of the internal rotation away from the equatorial plane (10–17).

Helioseismic data have revealed that the surface rotation rate persists through much of the convection zone on radial lines, and that there is a transition at or near the base of the convection zone to rotation that is independent of latitude. The sidereal rotation rate beneath the convection zone—roughly 440 nHz—is such that the latitudinally averaged specific angular momentum appears to be nearly constant across the convection zone boundary, which suggests that there is no net torque exerted across the transition (11, 18). The rotation in the radiative interior beneath the convective envelope seems to be consistent with rigid-body rotation. The rotation rate of the core is less certain; some reported low-degree splittings favor a rotation rate faster than the equatorial rate at the surface (8, 19), and others favor a somewhat slower rate (17, 20).

Helioseismic estimates of the pattern of rotation in the convection zone differ strikingly from predictions based on theoretical models. The convection in early numerical simulations of rotating convection in spherical shells was dominated by columnar roll-like cells orientated in the north-south direction. The tilting of these cells yielded Reynolds stress terms that drove zonal flows, which appeared as differential rotation (21). The convection models predicted that Ω was nearly constant along the axes of the columnar cells, and thus that angular velocity was nearly constant on cylinders aligned with the rotation axis and decreased with increasing depth in the equatorial plane. In contrast, the helioseismic data imply that angular velocity is roughly constant on radial lines. Recent numerical studies capable of describing more turbulent compressible flows have yielded more intricate profiles for Ω, although there is still some tendency for angular velocity to be constant on cylinders close to the equator (22). A likely explanation of the discrepancy between simulation and helioseismic inferences is that the spatial resolution in the theoretical convection models is capable of describing only mildly turbulent flows, whereas fully developed turbulence involving coherent structures embedded in otherwise chaotic flow fields may yield quite different mean flows and rotation profiles.

Interpreting Frequency Splittings

The splitting $\Delta\nu_{n\ell m}$ caused by the rotation $\Omega(r,\theta)$ can be written as

$$\Delta\nu_{n\ell m} = \frac{m}{2\pi}\int K_{n\ell m}(r,\theta)\Omega(r,\theta) r\, dr\, d\theta \quad (1)$$

where $K_{n\ell m}$ are weighting functions known as rotation kernels (Fig. 1). The kernels reflect the vertical and horizontal structure of the mode eigenfunctions. Because the spherical harmonics are either purely symmetric or purely antisymmetric about the equatorial plane, the amplitude of oscilla-

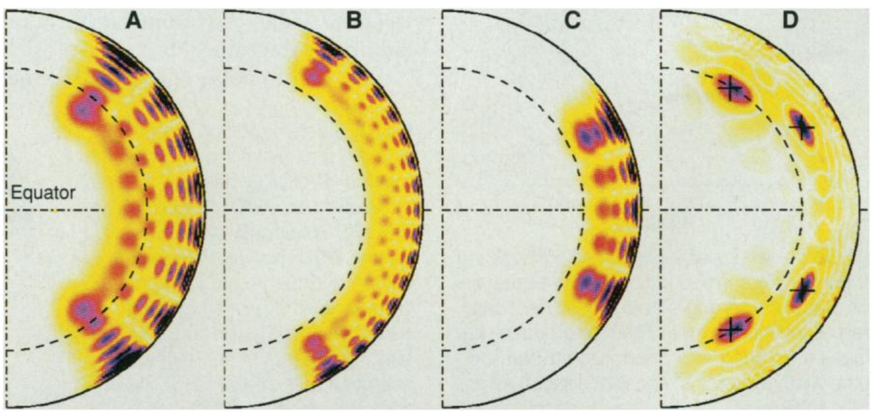

Fig. 1. (**A** to **C**) Meridional cuts through three rotation kernels for modes with frequencies $\nu \approx 1500$ μHz, for (A) $\ell = 15, m = 8$; (B) $\ell = 28, m = 14$; and (C) $\ell = 28, m = 24$. The color scale indicates the absolute magnitude of the kernel; dark colors (black and blue) represent the largest values, and light colors (yellow and white) represent values close to zero. The latitudinal extent of the kernels varies with m/L, and the radial extent varies with ν/L. Except close to the deepest point where it has appreciable amplitude, each kernel is nearly a product of a function of radius and a function of latitude. (**D**) Meridional cut through averaging kernels for a RLS inversion (as in Fig. 3B), for target radii and latitudes $r = 0.70R$, 60° and $r = 0.82R$, 30°. The averaging kernels are symmetric about the equatorial plane, so that they are also peaked at latitudes −60° and −30°. The four crosses indicate target locations.

tion is symmetric about the equator, and hence so too are the rotation kernels. Consequently, Eq. 1 implies that the splitting is sensitive only to that component of Ω that is symmetric about the sun's equatorial plane. Other contributions to the splitting might come from latitudinal variations in structure or from a magnetic field that is axisymmetric about the rotation axis. Such contributions are distinguishable from the rotation splitting because only the latter is antisymmetric in m.

Because the integrals of the rotation kernels are close to unity, the overall magnitude of the observed splittings readily provides an estimate of the sun's internal rotation rate. A simple way to proceed further would be to model the internal rotation profile with a few parameters, use Eq. 1 to compute the splittings corresponding to such a profile, and adjust the parameters to match the observed splittings. A more systematic approach would take account of the fact that different modes are sensitive to the rotation in different parts of the interior in a way that varies systematically with mode parameters. Modes sample the rotation rate in a cavity that extends from the surface down to a depth that increases with ν/L, where ν is the frequency of the mode and $L = \sqrt{\ell(\ell + 1)}$. Hence low-degree modes are sensitive to rotation from the surface to the core, whereas high-degree modes are only sensitive to the rotation close to the surface. In the latitudinal direction, modes sample the rotation between latitudes $\pm\cos^{-1}(m/L)$. Thus, the dependence of the splittings on ν/L and m/L may guide the construction of forward models for the rotation as a function of radius and latitude. For instance, splittings of modes with $m \approx \pm\ell$ show how the near-equatorial rotation varies with depth (Fig. 2). Each value of ν/L corresponds to a radius r_t to which such a mode penetrates, and thus the splitting represents a weighted average of the equatorial rotation between the surface and the radial location r_t. Thus the GONG data reveal that in the equatorial regions, as depth increases, the rotation rate first increases and then decreases. Suitable combinations of splittings sample the rotation rate at other latitudes (*23*). A data combination appropriate for a latitude of 30° (Fig. 2) shows that the sun rotates less rapidly at this latitude than at the equator, as is also observed from surface measurements. The rotation initially increases with increasing depth at this latitude, but this increase in rotation is less strong than at the equator.

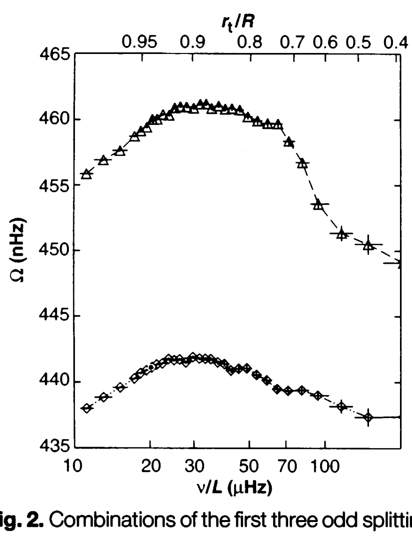

Fig. 2. Combinations of the first three odd splitting coefficients (*23*) corresponding to the equatorial region (upper curve) and latitude 30° (lower curve), plotted as functions of ν/L. The plotted points are averages over bins in ν/L; the horizontal bars indicate the width of the bins, and the vertical bars are the SD of the mean as calculated from the uncertainties in the individual splitting coefficients. These combinations are roughly weighted averages of the rotation (at each of the two latitudes) between the surface and the lower turning point radius r_t (top axis). The average rotation in the equatorial region is greater than at latitude 30°, and at both latitudes the rotation initially increases with increasing depth below the surface but decreases at greater depth.

Alternatively, various inverse techniques can be used; here we apply two such techniques to the GONG data. Suppose that it is possible to find a linear combination of the rotation kernels that is peaked at some chosen location within the sun and small elsewhere (Fig. 1). Because Eq. 1 is linear, the same linear combination of the measured splittings provides a weighted average of the internal rotation rate in the sun, weighted by the so-called averaging kernel. If the averaging kernel is localized, it yields an estimate of the rotation rate in some localized region of the solar interior. Repeating this process for different target locations yields a picture of the rotation rate inside the sun.

The construction of localized kernels is the essence of the optimally localized averages (OLA) method, also known as the Backus-Gilbert method (*24*, *25*). Another approach to inversion is to fit a parametric model of the internal rotation rate to the data with a least-squares fit. Because our problem is ill-conditioned, we use a regularized least-squares (RLS) method with a smoothing term that penalizes solutions that vary on small length scales. In our formulation, the solution at each point is a linear combination of the data, and thus it provides an estimate of the rotation rate as sampled by the corresponding linear combination of the rotation kernels, just as in OLA (*26*).

Inferences from GONG Data

Inversions of GONG splitting data by the OLA and RLS methods (Fig. 3), in the region where they can reasonably be determined with the 4-month data set, are in good agreement (*27–29*). In the convection zone above latitude ~30°, the data show that the rotation rate at a fixed latitude is roughly independent of depth, so that the variation with latitude is similar to that seen at the surface. Near the equator, the rotation rate increases just below the surface and reaches a maximum at roughly $r = 0.95R$ (where R is the radius of the sun). It then gradually decreases with increasing depth in the convective envelope. At the base of the convection zone near $r = 0.7R$, there is a pronounced transition at all latitudes to nearly uniform rotation at greater depths (Fig. 4). The structure of the transition is not resolved by the data. Thus, the GONG data support earlier deductions that the surface-like differential rotation is smoothed out near the base of the convection zone and that the rotation below this zone appears to become independent of latitude. The GONG data currently permit reliable inferences only to a depth of $r \approx 0.4R$, and the

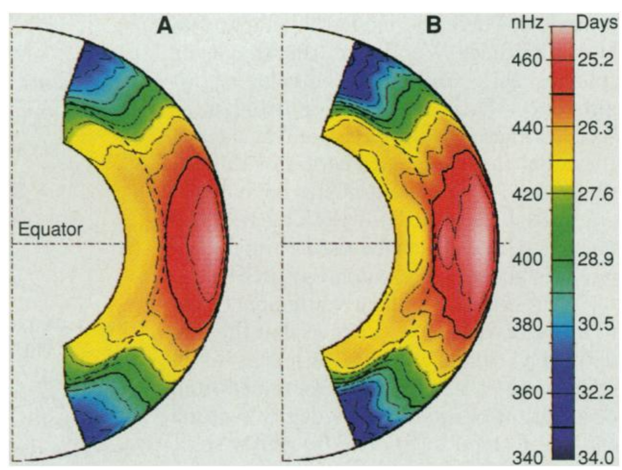

Fig. 3. Sidereal rotation rate inside the sun, as inferred from 4 months of GONG data on the basis of **(A)** an OLA 1 ⊗ 1 inversion (*25*, *28*) and **(B)** an RLS inversion (*29*). The color key indicates the rotation rate in nanohertz and the corresponding period in days. The contour spacing is 10 nHz; the highest contour line is at 460 nHz. The approximate base of the convection zone is indicated by the dashed line at $r = 0.7R$. The slightly more jagged appearance of the RLS solution results from a different balance between resolution and noise in the two inversions. Particularly noticeable is the local maximum in the rotation rate a little below the surface in the equatorial region. This shear layer appears to persist at least to mid-latitudes.

use of global modes yields little information near the poles (30). These inversions indicate the presence of two layers with strong horizontal shear in the mean azimuthal velocity, one positioned just below the surface and the other at the base of the convection zone. In contrast, gradients in Ω are mild in the rest of the convective envelope. These results are in accord with analyses of earlier helioseismic data. Our confidence in the inferences made from the nearly continuous GONG data is enhanced by the improved determination of frequency splittings with m, because GONG spectra do not suffer from daily side lobes, which plague single-site, ground-based observations.

The presence of an upper shear layer is consistent with the observation that at low latitudes, sunspots and supergranulation patterns rotate faster than does the surface gas (31). Perhaps near-surface convective motions with overturning times that are short relative to the rotation period (and thus are only mildly influenced by Coriolis forces) conserve their specific angular momentum as they move radially inward and toward the rotation axis, leading to a faster latitudinally dependent rotation rate than at the solar surface (32). Alternatively, recent numerical simulations of highly turbulent rotating convection within limited domains (33) exhibit prominent shear layers close to surfaces that bound the zone of convection, where the radial velocity vanishes and across which no net stresses are communicated. The convection models yield such shear layers only in the presence of intense turbulence that has ordered structures, and such turbulence has not yet been attained in models of convection in full spherical shells spanning a broader physical domain. Yet the real solar convection zone must be far more turbulent than any flows studied by simulation (22), and the added complexities of magnetic fields and the ionization zones of hydrogen and helium close to the surface of the convection zone must also be considered.

It has been conjectured that the combined presence of the ionization zones and the rapid variation in stratification near the surface may contribute to the lateral deflection of large-scale convective motions, possibly leading to substantial horizontal flows below the surface and only relatively feeble motions in the directly observable atmosphere. Such giant cells are expected to have horizontal dimensions comparable to the depth of the convecting shell. Giant cells have not yet been observed with any certainty, but the structure of the upper shear layer as inferred from helioseismic data, and the manner in which it varies with latitude, may eventually provide clues to the nature of coherent long-lived structured flows that may coexist with small-scale turbulence within the solar convection zone. The extent to which the shear layer extends to higher latitudes is uncertain from current observations that use the global modes; the inversions suggest that the shear changes sign at mid-latitudes (Fig. 3).

An alternative way of probing the upper shear layer is provided by helioseismic analyses of acoustic wave fields within a localized area, with the use of time-distance or ring-diagram methods (34). Ring analysis applied to some GONG data is shown in Fig. 5. If one-dimensional inversions in depth are performed, mosaics of such measurements can be used to map the mean flows with respect to depth beneath each patch. The local mean horizontal flows appear to spiral with increasing depth in the immediate subsurface layers, which suggests that the structure of shearing flows may be more intricate than that deduced from the properties of the global modes. Such local-area techniques would benefit from higher spatial resolution that future upgrades to GONG may provide.

The second shear layer at the base of the convection zone (Figs. 3 and 4) is a transition from the angular velocity profile of the convective envelope to a profile of possible solid-body rotation in the deeper radiative interior (35). This transition layer is likely to be dynamically complicated, for it is just below, or may even be part of, the overshooting region in which penetrating convective motions (probably in the form of discrete plumes) are rapidly decelerated as they encounter the stable stratification of the interior. Helioseismic findings that the radial gradient of the rotation rate is small in the convection zone itself have shifted attention to this transition layer as the site of the magnetic dynamo (36). To assess the properties of the region that is available for making and storing the magnetic fields, it would be helpful to know the nature of the stratification and the mean shearing flows achieved in the transition layer. However,

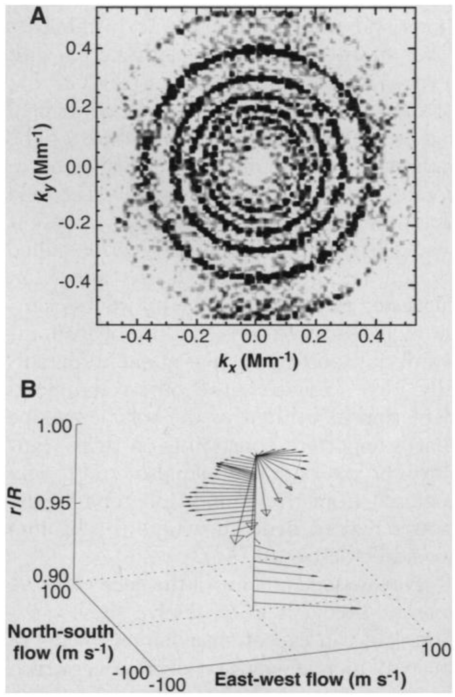

Fig. 5. Ring-diagram analysis of the superposition of local acoustic plane waves, each of which is advected locally by the horizontal component of the mean flow beneath the solar surface. The procedure here uses GONG multistation data in which a 45° subraster (involving 96^2 pixels and centered on the equator) is tracked at the solar rotation rate over a 56-hour interval. (**A**) Multiple rings (corresponding to different values of order n) are evident in the cut through the k_x-k_y-ν power spectrum at constant frequency ν = 3.5 mHz, where k_x and k_y are the eastward and northward components of the horizontal wave number. (**B**) The displacement of such rings can be used to infer the effective mean horizontal velocity sensed by the acoustic waves over a range of depths (34), shown as the spiraling set of arrows denoting amplitude and direction of this mean flow with respect to proportional radius r/R just below the surface.

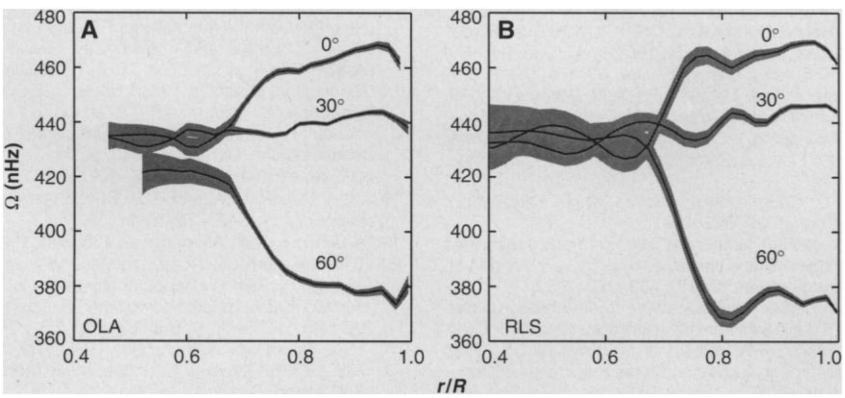

Fig. 4. Sections at latitudes 0°, 30°, and 60° through (**A**) the OLA inversion solution and (**B**) the RLS inversion solution (Fig. 3). Formal error bars (±1 SD) are indicated by the shaded regions (30). Both inversions indicate that surface-like differential rotation persists through the bulk of the convection zone, with a transition near the base of the convection zone to a flow that is consistent with latitudinally independent rotation.

inferences about the transition in rotation pattern and in mean stratification are still somewhat uncertain because of the resolution achieved in the inversions. With available data, the characteristic full width at half maximum (FWHM) of an averaging kernel peaked at low latitudes near the base of the convection zone is roughly $0.1R$, which is therefore essentially the radial resolution. However, forward modeling and inversions of artificial data indicate that the present inversion results are consistent with an abrupt transition (*37*). Beneath this transition layer, down to radius $0.4R$ where we can reliably make inferences with this data set, the rotation of the radiative interior appears to be much like that of solid-body rotation. However, although solid-body rotation may seem plausible because it represents the lowest energy state for a specified total angular momentum, it is uncertain how this state may be achieved within the sun. Models that incorporate the transport of angular momentum by slow circulations and their hydrodynamic instabilities favor an interior, and especially a core, with a rotation rate considerably faster than that of the solar surface (*1*). A weak connected magnetic field pervading the whole of the radiative interior could cause this region to rotate uniformly (*38*); presumably, the field does not penetrate the shear layer, where it would be stretched, but has been expelled by the turbulence (*39*). It has also been suggested that internal gravity waves excited by penetrative convection propagate inward, transporting angular momentum radially (*40*). However, the observed limited depletion of lithium in the solar envelope places important constraints on those spin-down processes that would also tend to mix material from the convection zone to the hotter regions beneath, where the lithium would be destroyed (*41*).

Helioseismic probing of the deep radiative interior should help to resolve these questions; we can expect great improvements in the resolution and range of depths over which we can make reliable inferences as we accumulate more data from GONG. Similar results to those in Figs. 3 and 4 have also been derived from the GONG data set by other inversion methods and by forward modeling; these results strengthen our conclusions regarding the rotation rate. It must be borne in mind that the rotation rate we have derived from the splittings of the global modes is a north-south symmetric average and an average over longitude and time. Moreover, the limited spatial resolution (*42*) results in smoothing of the inferred rotation rate of the sun. The examples of Jupiter and Saturn, which are likewise rotating, convecting bodies, suggest that the sun might have strong zonal jets and structured flows in addition to broader variations of differential rotation. Observing for longer periods will enable frequencies to be measured even more accurately, with consequent improved spatial resolution (*43*). However, the mean flows within the sun might not be steady over periods of a year or more; in that case, inverting time-averaged splitting data will only provide a picture of the time-averaged dynamics. The analyses of wave properties over more localized areas with the use of time-distance or ring-diagram approaches (*34*), both of which can be accomplished over shorter intervals in observing time, may serve as an important complement to the sampling afforded by the use of the global modes. The dynamics of the solar convection zone and deeper interior are likely to involve a diverse range of temporal and spatial scales of behavior (*22*), the resolution of which will require the extended imaging data sets that are now becoming available from GONG and associated helioseismic experiments.

REFERENCES AND NOTES

1. Rotational histories of low-mass stars like the sun are discussed in L. W. Hartmann and R. W. Noyes, *Annu. Rev. Astron. Astrophys.* **25**, 271 (1987); M. H. Pinsonneault, S. D. Kawaler, S. Sofia, P. Demarque, *Astrophys. J.* **338**, 424 (1989); B. Chaboyer, P. Demarque, M. H. Pinsonneault, *ibid.* **441**, 865 (1995).
2. Possible dynamical processes in the solar core are discussed in D. O. Gough, in *Solar-Terrestrial Relationships and the Earth Environment in the Last Millennium*, G. Castagnoli-Cini, Ed. (Soc. Italiana di Fisica, Bologna, 1988), pp. 90–132; W. J. Merryfield, J. Toomre, D. O. Gough, *Astrophys. J.* **367**, 658 (1991); S. Ghosal and E. A. Spiegel, *Geophys. Astrophys. Fluid Dyn.* **61**, 161 (1991). Computation of modifications to the neutrino flux is considered in D. O. Gough, *Ann. N.Y. Acad. Sci.* **647**, 119 (1991).
3. The average sidereal rotation rate $\Omega/2\pi$ from photospheric Doppler measurements is ~452 nHz at the equator, 432 nHz at 30°, and 369 nHz at 60° [R. K. Ulrich *et al.*, *Sol. Phys.* **117**, 291 (1988)]. The rotation rate determined by tracking sunspots varies with the size of the spot group [R. Howard, P. A. Gilman, P. I. Gilman, *Astrophys. J.* **283**, 373 (1984)] or with the age of the spots [E. Nesme-Ribes *et al.*, *Astron. Astrophys.* **274**, 563 (1993)]. Average sunspot rotation rates are 467 nHz and 465 nHz, respectively, near the equator, and 444 nHz and 450 nHz at 30°. See also E. H. Schröter, *Sol. Phys.* **100**, 141 (1985).
4. P. A. Gilman, in *Physics of the Sun*, P. A. Sturrock, T. E. Holzer, D. M. Mihalas, R. K. Ulrich, Eds. (Reidel, Dordrecht, Netherlands, 1986), vol. 1, pp. 95–160; S. K. Solanki, *Space Sci. Rev.* **63**, 1 (1993); F. Cattaneo, in *Solar Magnetic Fields*, M. Schüssler and W. Schmidt, Eds. (Cambridge Univ. Press, Cambridge, 1993), pp. 261–275; P. R. Wilson, *Solar and Stellar Activity Cycles* (Cambridge Univ. Press, Cambridge, 1994).
5. D. O. Gough and J. Toomre, *Annu. Rev. Astron. Astrophys.* **29**, 627 (1991).
6. The effect of large-scale flows on mode frequencies and linewidths is discussed by E. M. Lavely and M. H. Ritzwoller, *Astrophys. J.* **403**, 810 (1993).
7. Low-degree oscillations were studied through Doppler shifts in light from the entire solar disk (*8*) [G. Grec, E. Fossat, M. A. Pomerantz, *Sol. Phys.* **82**, 55 (1983)] and through fluctuations in the limb-darkening function [H. Hill, R. J. Bos, P. R. Goode, *Phys. Rev. Lett.* **49**, 1794 (1982)].
8. A. Claverie *et al.*, *Nature* **293**, 443 (1981).
9. Sectoral modes were studied with a cylindrical lens that folded the solar image into the entrance slit of a spectrograph aligned with the solar equator [T. L. Duvall Jr. and J. W. Harvey, *Nature* **310**, 19 (1984)], and splitting data were inverted (T. L. Duvall Jr. *et al.*, *ibid.*, p. 22).
10. Frequency splittings for intermediate-degree modes were done with the Fourier Tachometer, the progenitor of the GONG instrument [T. M. Brown and C. A. Morrow, *Astrophys. J.* **314**, L21 (1987)], and the data were inverted [(*11*); see also T. M. Brown, *Nature* **317**, 591 (1985)].
11. T. M. Brown *et al.*, *Astrophys. J.* **343**, 526 (1989).
12. Intermediate-degree frequencies and splittings from Big Bear Solar Observatory, using Doppler imaging with a tunable birefringent filter, were reported for a 1986 campaign [K. G. Libbrecht, *Astrophys. J.* **336**, 1092 (1989)], with further campaigns during 1988–1990 [K. G. Libbrecht and M. F. Woodard, *Nature* **345**, 779 (1990); M. F. Woodard and K. G. Libbrecht, *Astrophys. J.* **402**, L77 (1993)]. For discussions of rotation inversions, see J. Christensen-Dalsgaard and J. Schou, in *Seismology of the Sun and Sun-Like Stars*, E. J. Rolfe, Ed. (ESA SP-286, ESA, Noordwijk, Netherlands, 1988), pp. 149–153; W. A. Dziembowski, P. R. Goode, K. G. Libbrecht, *Astrophys. J.* **337**, L53 (1989); D. O. Gough *et al.*, *Astron. Soc. Pac. Conf. Ser.* **40**, 93 (1993); M. F. Woodard and K. G. Libbrecht, *Science* **260**, 1778 (1993).
13. Intermediate- and high-degree mode parameters deduced from South Pole Ca II intensity observations were reported in T. L. Duvall Jr., J. W. Harvey, M. A. Pomerantz, *Nature* **321**, 500 (1986); T. L. Duvall Jr. *et al.*, *Astrophys. J.* **324**, 1158 (1988); T. L. Duvall Jr., J. W. Harvey, S. M. Jefferies, M. A. Pomerantz, *ibid.* **373**, 308 (1991); S. M. Jefferies *et al.*, *ibid.* **377**, 330 (1991); T. L. Duvall Jr. *et al.*, *ibid.* **410**, 829 (1993). The most recent South Pole instrumentation now serves as the High Degree Helioseismometer (HDH) [K. T. Bachmann, T. L. Duvall Jr., J. W. Harvey, F. Hill, *ibid.* **443**, 837 (1995)].
14. Extensive sets of intermediate- and high-degree frequencies and splittings observed from Mount Wilson with a Doppler magneto-optical analyzer have been reported [S. Tomczyk *et al.*, in *Seismology of the Sun and Sun-Like Stars*, E. J. Rolfe, Ed. (ESA SP-286, ESA, Noordwijk, Netherlands, 1988), pp. 141–147], and the data have been inverted [S. G. Korzennik *et al.*, *ibid.*, pp. 117–124; E. J. Rhodes Jr. *et al.*, *Astrophys. J.* **351**, 687 (1990)]. For inferences from 1988 and 1990 campaigns, see S. G. Korzennik *et al.*, in *Proceedings of the Oji International Seminar Progress of Seismology of the Sun and Stars*, Y. Osaki and H. Shibahashi, Eds. (Springer-Verlag, Berlin, 1990), pp. 341–348; P. R. Goode *et al.*, *Astrophys. J.* **367**, 649 (1991); S. G. Korzennik, A. Cacciani, E. J. Rhodes Jr., *Astron. Soc. Pac. Conf. Ser.* **42**, 201 (1993); S. G. Korzennik *et al.*, *ibid.* **76**, 12 (1995).
15. The low- and intermediate-degree (LOWL) magneto-optical analyzer [S. Tomczyk *et al.*, *Sol. Phys.* **159**, 1 (1995)] has produced a long campaign of observations from Mauna Loa, Hawaii. For rotation inversions, see S. Tomczyk, J. Schou, M. J. Thompson, *Astrophys. J.* **448**, L57 (1995).
16. Recent interpretations of low-ℓ splittings have been reported from the International Research on the Interior of the Sun (IRIS) network [E. Fossat *et al.*, *Astron. Soc. Pac. Conf. Ser.* **76**, 24 (1995)], from the Birmingham Solar Oscillation Network (BiSON) (Y. Elsworth *et al.*, *ibid.*, p. 43) (*17*), and from the Interplanetary Helioseismology by Irradiance (IPHIR) measurements (T. Toutain, *ibid.*, p. 34).
17. Y. Elsworth *et al.*, *Nature* **376**, 669 (1995).
18. W. A. Dziembowski and P. R. Goode, *Astron. Soc. Pac. Conf. Ser.* **42**, 225 (1993).
19. A. Jiménez *et al.*, *Astrophys. J.* **435**, 874 (1994).
20. T. Toutain and A. G. Kosovichev, *Astron. Astrophys.* **284**, 265 (1994); T. Appourchaux *et al.*, in *Fourth SOHO Workshop Helioseismology*, T. Hoeksema, V. Domingo, B. Fleck, B. Battrick, Eds. (ESA SP-376, ESA, Noordwijk, Netherlands, 1995), vol. 2, pp. 265–270; S. Tomczyk, J. Schou, M. J. Thompson, *Bull. Astron. Soc. India*, in press.
21. For numerical simulations of convection constrained by rotation within spherical shells, see G. A. Glatzmaier, *Astrophys. J.* **291**, 300 (1985); P. A. Gilman and J. Miller, *Astrophys. J. (Suppl.)* **61**, 585 (1986); G. A. Glatzmaier, in *The Internal Solar Angular Velocity*, B. R. Durney and S. Sofia, Eds. (Reidel, Dord-

recht, Netherlands, 1987), pp. 263–274. Modified mixing-length and anisotropic-diffusion models can also be used to estimate Reynolds stresses of rotating convection [G. Rüdiger, *Geophys. Astrophys. Fluid Dyn.* **16**, 239 (1980); G. Belvedere, L. Paterno, M. Stix, *Astron. Astrophys.* **86**, 40 (1980); D. H. Hathaway, *Astrophys. J.* **276**, 316 (1984); B. R. Durney, *ibid.* **378**, 378 (1991)].

22. N. Brummell, F. Cattaneo, J. Toomre, *Science* **269**, 1370 (1995); G. A. Glatzmaier and J. Toomre, *Astron. Soc. Pac. Conf. Ser.* **76**, 200 (1995).
23. The m dependence of the splittings for given n and ℓ can be approximately parameterized by a low-order polynomial in m/L,

$$\Delta\nu_{n\ell m} = \sum_{k=1}^{N} a_k(n,\ell)\mathcal{P}_k^{(\ell)}(m) \qquad (2)$$

where $\mathcal{P}_k^{(\ell)}(m)$ are polynomials in m of degree k; a common choice is $\mathcal{P}_k^{(\ell)}(m) = LP_k(m/L)$, where P_k is a Legendre polynomial. The coefficients a_k then depend on the number N of terms included in the expansion. We used orthogonal polynomials (*44*) [M. H. Ritzwoller and E. M. Lavely, *Astrophys. J.* **369**, 557 (1991)] that are asymptotically equal to the previous choice of polynomials and yet make the coefficients almost independent of N. The traces in Fig. 2 show $a_1 + a_3 + a_5$ (equatorial) and $a_1 - {}^1/_4(a_3) - {}^{19}/_{16}(a_5)$ (latitude 30°). Further details of the combining of data are given in (*11*) and in P. R. Wilson and D. Burtonclay, *Astrophys. J.* **438**, 445 (1995).
24. The combining of kernels as in OLA was introduced by G. Backus and F. Gilbert [*Geophys. J. R. Astron. Soc.* **16**, 169 (1968); *Philos. Trans. R. Soc. London Ser. A* **266**, 123 (1970)]. Its use in helioseismology is discussed in D. O. Gough, *Sol. Phys.* **100**, 65 (1985); the particular formulation known as SOLA is discussed in F. P. Pijpers and M. J. Thompson, *Astron. Astrophys.* **262**, L33 (1992).
25. OLA is computationally expensive, requiring the inversion of a matrix, the order of which is equal to the number of data. The 1 ⊗ 1 inversion approach we use [T. Sekii, *Mon. Not. R. Astron. Soc.* **264**, 1018 (1993); in *Fourth SOHO Workshop Helioseismology*, T. Hoeksema, V. Domingo, B. Fleck, B. Battrick, Eds. (ESA SP-376, ESA, Noordwijk, Netherlands, 1995), vol. 2, pp. 285–288] is much less expensive because it exploits the fact that the kernels are approximately the product of a function of radius and a function of latitude (Fig. 1).
26. The RLS fit minimizes the sum of the squared residuals (the χ^2 misfit) between the data and the splittings predicted by the parameterized model, plus a function that penalizes solutions that are large or that vary on small length scales. The competing misfit and regularity of the solution are balanced by a trade-off parameter [see I. J. D. Craig and J. C. Brown, *Inverse Problems in Astronomy* (Hilger, Bristol, UK, 1986)].
27. The data were splitting coefficients a_i (i = 1, 3, . . . , 17) averaged over 4 months, for 957 (n,ℓ) multiplets in the ranges ℓ = 3 to 178 and ν = 1500 to 3500 μHz. Splittings were determined separately for each of GONG months 1, 2, 4, and 5, and these were then averaged with equal weights.
28. A SOLA inversion in latitude is performed for each degree ℓ to localize the angular kernels $[P_\ell^m(x)]^2$, where P_ℓ^m is an associated Legendre function and $x = \cos\theta$. The chosen target function, which is normalized to have unit area, is a sum of two Gaussians, one centered at x_0 and the other at $-x_0$. Once the angular inversion coefficients $\beta_{\ell m}$ are obtained, the quantities $F_{n\ell} = \sum_m \beta_{\ell m}\Delta\nu_{n\ell m}$ are computed and stored. (For the inversion presented here, splitting coefficients were used instead of $\Delta\nu_{n\ell m}$, but the principle is the same.) Radial inversion coefficients $c_{n\ell}$ for target location r_0 are determined by minimizing an integral over r and x of the square of the averaging kernel, weighted by $(r - r_0)^2(x - x_0)^2$. Finally, the rotation rate estimate is obtained as $\sum_{n\ell} c_{n\ell}F_{n\ell}$.
29. The implementation of the RLS inversion was as described in (*44*), with second-derivative smoothing in both radial and latitudinal directions. We obtained similar results using first-derivative smoothing in the latitudinal direction. The values of the trade-off parameters in the two directions were chosen to be $\mu_r = 10^{-6}$, $\mu_\theta = 10^{-5}$ so as to give a reasonable trade-off between resolution and variance of the solution. More automated procedures for selecting values for the trade-off parameters, such as generalized cross-validation, are available.
30. The formal 1σ error bars in Fig. 4 indicate how the solution at a point would vary given different realizations of the data noise. They do not necessarily provide a confidence interval that covers the true solution because of the finite resolution of the inversion. Specifically, in the RLS the choice of finite basis and the smoothing penalty term both introduce biases. It is possible to estimate the magnitude of the latter effect by computing the terms in an expansion about the estimated parameters, but we have not done so here.
31. T. L. Duvall Jr., *Sol. Phys.* **66**, 213 (1980).
32. P. Foukal and J. R. Jokipp, *Astrophys. J.* **199**, L71 (1975); P. Foukal, *ibid.* **218**, 539 (1977); P. A. Gilman and P. V. Foukal, *ibid.* **229**, 1179 (1979).
33. N. H. Brummell, X. Xie, J. Toomre, C. Baillie, *Astron. Soc. Pac. Conf. Ser.* **76**, 192 (1995); J. Toomre and N. H. Brummell, in *Fourth SOHO Workshop Helioseismology*, T. Hoeksema, V. Domingo, B. Fleck, B. Battrick, Eds. (ESA SP-376, ESA, Noordwijk, Netherlands, 1995), vol. 1, pp. 47–62; N. H. Brummell, N. E. Hurlburt, J. Toomre, *Astrophys. J.*, in press.
34. Time-distance methods based on studies of acoustic travel time along sets of ray paths may eventually enable mapping of localized structures in wave speed and flow velocities, as discussed for HDH data from the South Pole [T. L. Duvall Jr., S. M. Jefferies, J. W. Harvey, M. A. Pomerantz, *Nature* **362**, 430 (1993); T. L. Duvall Jr., S. D'Silva, S. M. Jefferies, J. W. Harvey, J. Schou, *ibid.* **379**, 235 (1996)] and with inversion of maps of travel times [A. G. Kosovichev, *Astrophys. J.* **461**, L55 (1996)]. Ring-diagram analysis involves observing the wave fields while tracking localized regions on the sun to deduce the average horizontal flows and sound-speed perturbations beneath the region [F. Hill, *Astrophys. J.* **333**, 996 (1988); *Sol. Phys.* **128**, 321 (1990); *Astron. Soc. Pac. Conf. Ser.* **76**, 484 (1995)]. Data about the displacement of the rings evident in slices at fixed frequency in the power spectra have been inverted [J. Pátron *et al.*, *Astrophys. J.* **455**, 746 (1995)].
35. The transport of angular momentum within the convection zone and in an adjustment layer at its base is discussed in P. A. Gilman, C. A. Morrow, E. E. DeLuca, *Astrophys. J.* **338**, 528 (1989). The properties of a turbulent "solar tachocline" to achieve a transition in the rotation rate of the convection zone to that of the deeper interior are discussed in E. A. Spiegel and J.-P. Zahn, *Astron. Astrophys.* **265**, 106 (1992), assuming that the helioseismically inferred rotation profile of the convection zone must adjust rapidly in radius to the interior state while transferring little or no net torque. If shear instabilities in the adjustment layer lead to substantial turbulent diffusive processes in the horizontal that can balance the advection of angular momentum, then a thin transition region can result.
36. E. A. Spiegel and N. O. Weiss, *Nature* **287**, 616 (1980); R. Rosner, in *Cool Stars, Stellar Systems, and the Sun*, A. K. Dupree, Ed. (SAO SR-389, Smithsonian Astrophysical Observatory, Cambridge, 1980), pp. 79–96; L. Golub, R. Rosner, G. S. Vaiana, N. O. Weiss, *Astrophys. J.* **243**, 309 (1981); G. A. Glatzmaier, *Geophys. Astrophys. Fluid Dyn.* **31**, 137 (1985); D. Schmitt, in *The Cosmic Dynamo*, F. Krause, K.-H. Rädler, G. Rüdiger, Eds. (Kluwer, Dordrecht, Netherlands, 1993), pp. 1–12.
37. The finite resolution smooths out even discontinuous transitions [see M. J. Thompson, *Sol. Phys.* **125**, 1 (1990)]. Techniques more appropriate for detecting sharp features include looking directly for the signature of a discontinuity or jet stream [D. O. Gough, in *Proceedings of the Oji International Seminar Progress of Seismology of the Sun and Stars*, Y. Osaki and H. Shibahashi, Eds. (Springer-Verlag, Berlin, 1990), pp. 283–318] and designing averaging kernels that are sensitive to sharp gradients or local extrema [F. P. Pijpers and M. J. Thompson, *Astron. Soc. Pac. Conf. Ser.* **42**, 241 (1993)].
38. R. Rosner and N. O. Weiss, *Nature* **317**, 790 (1985); L. Mestel and N. O. Weiss, *Mon. Not. R. Astron. Soc.* **226**, 123 (1987); P. Charbonneau and K. B. MacGregor, *Astrophys. J.* **417**, 762 (1993).
39. N. O. Weiss, *Proc. R. Soc. London Ser. A* **293**, 310 (1966).
40. J.-P. Zahn, *Astron. Astrophys.* **288**, 829 (1994).
41. E. Schatzman, *Astrophys. Lett.* **3**, 139 (1969); *Astron. Astrophys.* **56**, 211 (1977); J.-P. Zahn, *ibid.* **265**, 115 (1992).
42. A measure of the local resolution is the width of the main peak of the averaging kernels. We estimate the radial and latitudinal resolution by fitting to each averaging kernel a double Gaussian with widths w_r and w_θ in radius and latitude, plus its mirror image in the equatorial plane (*44*). The widths of some representative averaging kernels for the RLS inversion illustrated in Figs. 3B and 4B are as follows: $w_r = 0.06R$, $w_\theta = 0.11R$ at $r = 0.70R$, 60°; $w_r = 0.05R$, $w_\theta = 0.10R$ at $r = 0.70R$, 30°; $w_r = 0.025R$, $w_\theta = 0.10R$ at $r = 0.91R$, 30°. The FWHM in each direction is larger than these values by roughly a factor of 1.7.
43. J. Christensen-Dalsgaard, J. Schou, M. J. Thompson, J. Toomre, *Astron. Soc. Pac. Conf. Ser.* **76**, 212 (1995); in *Fourth SOHO Workshop Helioseismology*, T. Hoeksema, V. Domingo, B. Fleck, B. Battrick, Eds. (ESA SP-376, ESA, Noordwijk, Netherlands, 1995), vol. 2, pp. 41–45.
44. J. Schou, J. Christensen-Dalsgaard, M. J. Thompson, *Astrophys. J.* **433**, 389 (1994).
45. Supported by the UK Particle Physics and Astronomy Research Council, NSF, NASA, Danmarks Grundforskningsfond, CNRS, and the Institut du Développement et des Ressources en Informatique Scientifique, France. GONG is managed by NSO, a division of NOAO that is operated by the Association of Universities for Research in Astronomy under cooperative agreement with NSF.

18 March 1996; accepted 9 May 1996